Novel Design and Implementation of MIMO Antenna for LTE Application

Mowafak. K. Mohsen[1,4], M.S.M Isa[1], T.A. Rahman[2], M. K. Abdulhameed[1,4], A.A.M.Isa [1], M.S.I.M.Zin[1] S.Saat[1], Z.Zakaria[1], I.M.Ibrahim[1], M.Abu[1], A.Ahmad[3]
[1]*Center for Telecommunication Research and Innovation(CeTRI), Faculty of Electronic and Computer Engineering, Universiti Teknikal Malaysia Melaka, Malaysia*
[2]*Faculty of Electrical Engineering, Universiti Teknologi Malaysia, 81310 UTM Skudai, Johor, Malaysia.*
[3]*Faculty of Information and Communication Technology, Universiti Teknikal Malaysia Melaka, Jalan Hang Tuah Jaya, 75300, Melaka*
[4]*Ministry of Higher Education and Scientific Research, Baghdad, Iraq*
saari@utem.edu.my

***Abstract*—The quest for achieving high bandwidth connectivity that renders a complete wireless system ideal for video-intensive applications at very low power consumption using multiple inputs/multiple outputs (MIMO) dual-band combo chip with high-speed is ever-growing. A newly designed structure of the MIMO antenna four ports is implemented for efficient bandwidth broadening. The bandwidth and S-parameters of the antenna are simulated and determined. The dual-band MIMO micro-strip patch antenna comprised of four ports where the ground plane is extruded on a substrate having area 125x128 mm^2 and thickness 1.6 mm. The antenna is fabricated on an inexpensive FR4 with the dielectric constant of 4.5, loss tangent ~0.019 and patch thickness of 0.035 mm. The MIMO antenna with dimension 53.5x38.25 mm^2 operates at 1.8 and 2.6 GHz. The proposed antenna is found to achieve good pattern diversity, low correlation coefficient, high gain, excellent directivity, and quite reasonable bandwidth in the above-mentioned range, highly suitable for LTE bands application with 10 dB return loss. The CST microwave studio program is used for the simulation, and real experimental measurements are made using Agilent Technologies E5071B VNA and the equipment inside the anechoic chamber. Measurements on the prototype antenna are carried out, and characteristic evaluations are performed for comparison. The admirable features of the results suggest that our systematic approach may constitute a basis for the design and implementation of MIMO antenna for diverse LTE applications.**

***Index Terms*—Dual band; Four Port Antenna; LTE; MIMO.**

I. INTRODUCTION

Lately, the Multiple-Input Multiple-Output shortly called MIMO technology using multiple antennas at both the transmitter and receiver in improving the communication performance by transferring more data at the same time has gained tremendous attention. It is one of the several forms of smart antenna technology [1]. The optimal performance and range of MIMO require the support of both the station (mobile device) and the access point. It is well known that MIMO technology takes advantage of a natural radio-wave phenomenon called multipath where the transmitted information bounces off walls, ceilings, and other objects, reaching the receiving antenna multiple times via different angles and at slightly different times [2,3]. The MIMO simply supplies real communication in terms of multi-antenna wireless channels to wireless digital subscriber lines. Its performance is measured using the cross-correlation coefficients between the received signals by different antenna elements. Therefore, the aim is to minimize the correlation coefficient between the antenna elements to maximize the capacity. Furthermore, the MIMO has the attribute of being able to solve the enhancement of the communication capacity of band-limited wireless systems [4,5]. MIMO system. The proposed optimization method is further employed to acquire the most favorable positions of two antenna elements that minimize the cross-correlation coefficients, leading to efficient MIMO operation [4,6].

Diversity in current LTE systems is usually restricted to two antennas for each radio, which sufficiently ensures that if one antenna is in an RF null, the other is generally not, thereby provides better performance in multipath environments. Antenna diversity is already being used with LTE for countering multipath, reducing outage, improving the quality and reliability of the communications link [7-9]. Generally, three types of diversity are used. Firstly, two antennas can be deployed as far apart as possible to create some spatial diversity. Secondly, they can be oriented orthogonal to give polarization diversity. Lastly, they can possess different beams patterns [10,11]. A MIMO system often uses four antennas that make it more powerful than diversity switching in improving communications link. The technique is far more robust and can be improved further by employing a larger number of antennas than those used. In addition, an optimal subset can be selected on the basis of channel quality. In this system, only one radio is present where the receiver listens to one antenna at a time, and an RF switch is used to select the antenna producing the best signal. Despite such efforts, the widespread commercialization of such antennas is far from being realized [12,13].

The design and implementation of a new type of MIMO micro-strip patch antenna consisting of four ports which are capable of broadening the bandwidth have been reported. The bandwidth, S-parameters, gain, and correlation coefficients are determined to examine the efficiency [14]. The characteristic evaluations are performed via the simulation using CST microwave studio program; the results are analyzed and compared [15,16].

II. METHODOLOGY

It is worth mentioning that the element of the MIMO antenna, the dual-band microstrip patch is chosen due to its ease manipulation and facile configuration. The computation of the optimum patch dimension is executed at the preferred frequency where the line of the microstrip is used as a feeding mechanism for energy excitation. CST Microwave Studio 2010 is used on an optimum dimension of all elements, and the microstrip line is fed to simulate the antenna loss. The optimized simulation MIMO antenna is fabricated using a wet etching process and followed by the measurement process and further analyses. Figure 1 to 3 displays the real dimensions and geometrical parameters of the elements (front and rear views) used on the substrate designed via the CST microwave studio.

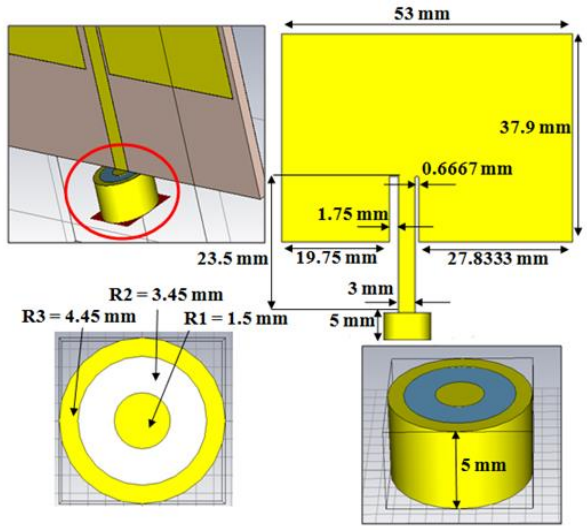

Figure 1: Geometric dimensions of CST Microwave Studio designed dual band antenna (enclosed in the red circle) operating at frequency 1.8 and 2.6 GHz for LTE application.

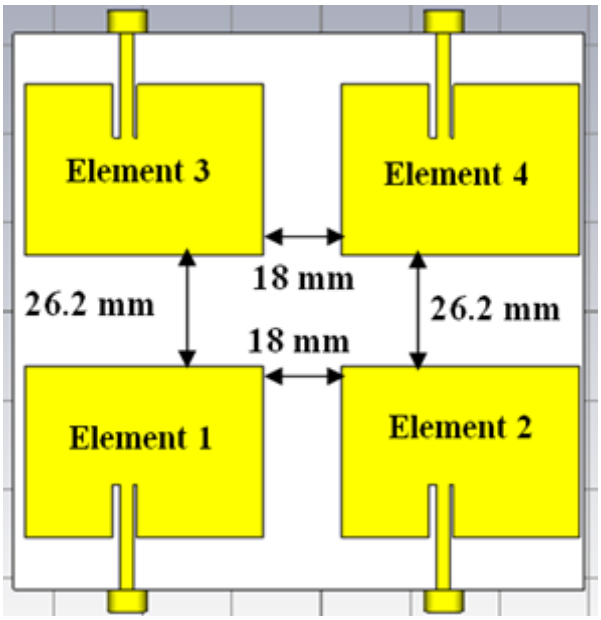

Figure 2: Front view of the MIMO 4-ports dual band antenna.

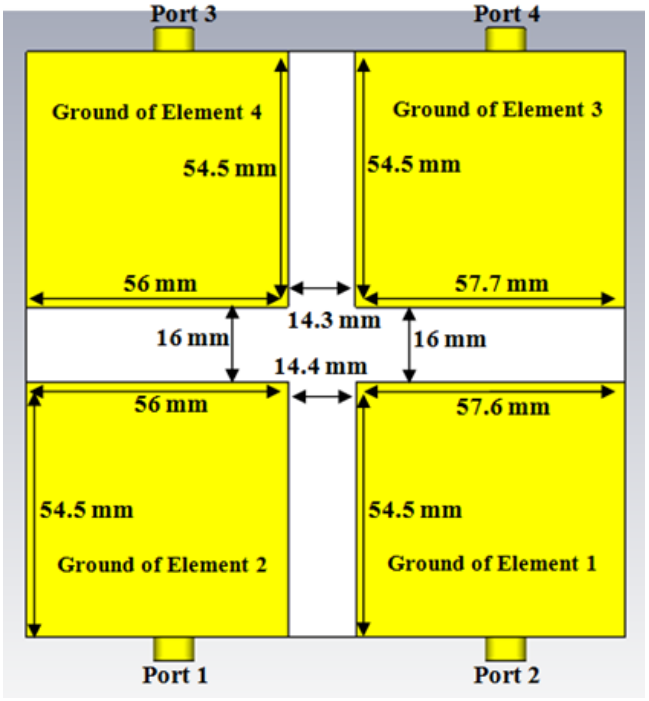

Figure 3: Rear view of the MIMO 4 ports dual band antenna.

The finite domain time integration analyses of electromagnetic (EM) waveguide the microstrip patch antenna (MPA) dual band as MIMO 4 port is simulated at frequency 1.8 and 2.6 GHz. Excitation of MIMO antenna is triggered via adjacency coupling between antenna 1, 2, 3 and 4 that generates the magnetic field in the microstrip patch dual band to produce the short horizontal magnetic signal. Figure 4 illustrates the design of a microstrip patch antenna having unequal slot dimensions between the fed.

A comparison of the return loss of dual-band the microstrip patch antenna, without and with equal dimensions of a slot between feeding line reveal a bandwidth of 6% and 2.5%, respectively. This is achieved without any optimization, and the same feeding technique is applied as illustrated in Figure 4. The former one performs better than the previous configuration. This difference in performance is attributed to the radiation only through the patch in the former case in comparison to the microstrip patch antenna radiation through the entire boundary of the dielectric-free space surface except for the grounded one for the latter configuration.

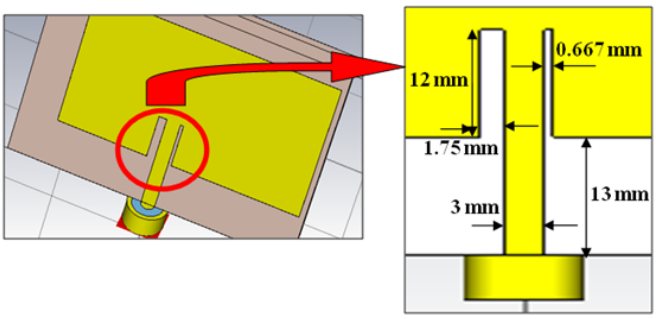

Figure 4: Microstrip Patch Antenna (MPA) with unequal dimensions of slot between fed lines.

III. PROTOTYPE FABRICATION

Computer Numerical Control (CNC) machine is used to cut the microstrip patch antenna in the desired dimension along x, y, and z-direction by maintaining their consistency and quality. The machine is abstractly programmed via a postprocessor with commands encoded on a storage medium for precise operation. This is highly significant for the dissection of the MPA dimensions and the manufacturing flow of the combined four antennas printed board. The wet etching process is used to fabricate feed line printed board to etch plane and a microstrip feed line to the other side of the board. The probe/SMA connector is properly soldered to the feed line of MPA. Finally, the unused resist is eliminated, and a smooth surface is obtained by rubbing through a sand paper. Fabrication of the whole processes includes the wet etching, the UV exposure, and the developing stages. The frequency dependent return loss (reflection coefficient) of the antenna as shown in Figure 5 is simulated by the transient solver in CST Microwave Studio between 1.8 and 2.6 GHz. The return loss bandwidth for inset-fed MPA is found to be ~2.5% (<5%) over the entire frequency range. Table 1 summarizes the results of return loss at two different operating frequencies for the simple printed dual-band planar antenna suitable towards LTE application.

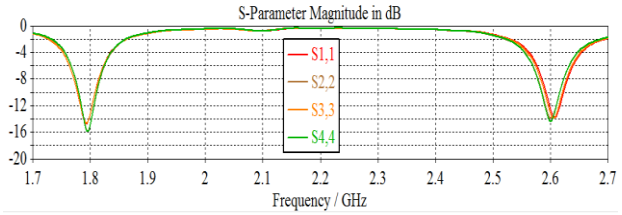

Figure 5: Simulated reflection coefficients for each port of the proposed MIMO antenna.

The value of return loss at the two resonant frequencies 1.8GHz and 2.6GHz are found to be -14.8dB and -13.5 dB respectively. These values meet the design requirement which is less than -10 dB, indicating that more than 90% of the fed power is absorbed. Simulation achieves satisfactory bandwidths of 19% and 12%, which are sufficient to cover the dual frequencies (1.8GHz and 2.6 GHz) span of LTE. The acquired 10 dB bandwidth at the two frequencies give 19% and 15.6% of return loss which is better than the measured. The simulation results for MIMO isolation parameters at frequencies 1.8GHz and 2.6 GHz are listed in Table 2. Figure 6 depicts the frequency dependent correlation coefficients for all values of isolation parameters between antennas.

Table 1
Values of Return Loss at Two Different Operating Frequencies.

Operating Frequency (GHz)	Return Loss (dB)			
	S_{11}	S_{22}	S_{33}	S_{44}
1.8	-13.500	-14.806	-13.902	-14.806
2.6	-13.323	-13.462	-13.281	-13.461

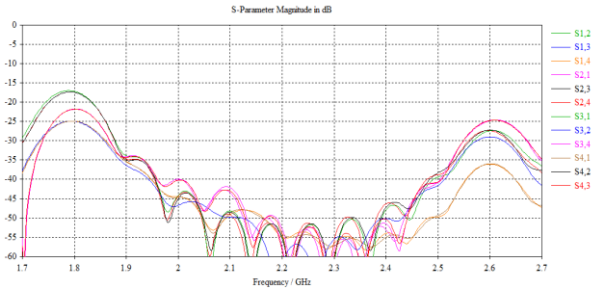

Figure 6: Frequency dependent reflection coefficients for all isolation parameters of 4-Port MIMO antenna.

Table 2
Results for Isolation Parameters

Isolation Parameter Description	Return Loss (dB) at 1.8GH	Return Loss (dB) at 2.6GHz
S_{12}	-22.0991	-25.4532
S_{13}	-17.0300	-30.5071
S_{14}	-25.0822	-30.7130
S_{21}	-21.8751	-25.4521
S_{23}	-25.1060	-30.7300
S_{24}	-17.2530	-32.3111
S_{31}	-17.0132	-30.5000
S_{32}	-25.0821	-30.7520
S_{34}	-21.8691	-25.4831
S_{41}	-25.1063	-30.7522
S_{42}	-17.2531	-32.3374
S_{43}	-21.8751	-25.4500

IV. RESULTS AND DISCUSSION

The designed prototype 4-ports MIMO antenna is displayed in Figure 7. E5071C ENA Series Network Analyzer is used to measure antenna return loss as shown in Figure 7, the key features of this analysis 2- or 4-port, 50ohm, S-parameter test set and Improve accuracy, yield and margins with wide dynamic range 130 dB, fast measurement speed 8ms and excellent temperature stability 0.005 dB/°C For the radiation pattern measurement, it has to be tested in an anechoic chamber. An anechoic chamber is a room with the interior surfaces covered with radiation absorbed (RAM) designed to stop reflections of electromagnetic wave Measurements are made with the antenna; data are analyzed and compared with the simulated results. Figure 8 shows a comparison between measured and simulated values of return loss of the antenna as a function of bandwidth frequency response for port 2 (S_{22}), respectively. The resonance frequency for the S_{22} parameter at both 2.6GHz and 1.8GHz exhibits the same level of an upward shift of 45MHz. The experimental and simulation results for the bandwidth of the prototype are approximately similar (36%). It is important to mention that the resonance antenna is dual in nature where the measured result of the first resonance is shifted to the lower frequency of 1.7GHz instead of 1.8 GHz creating a band which not covered in the proposed bandwidth.

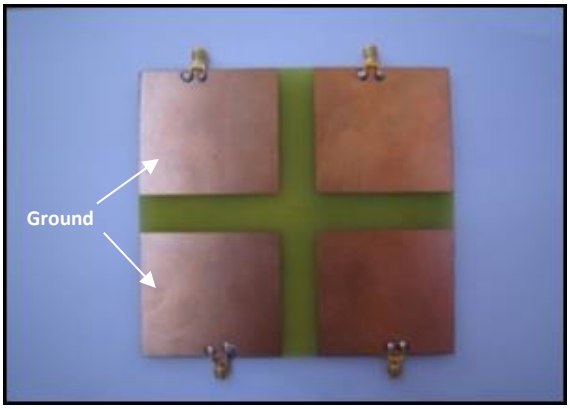

(a)

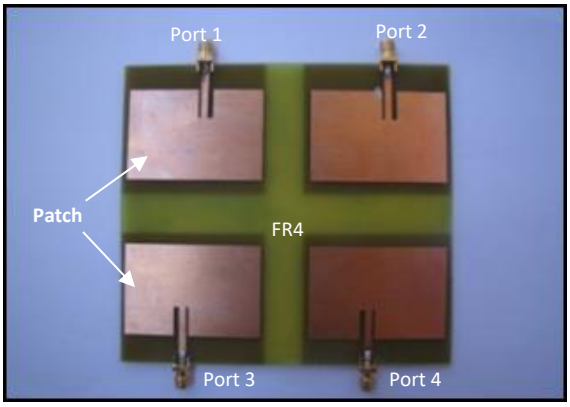

(b)

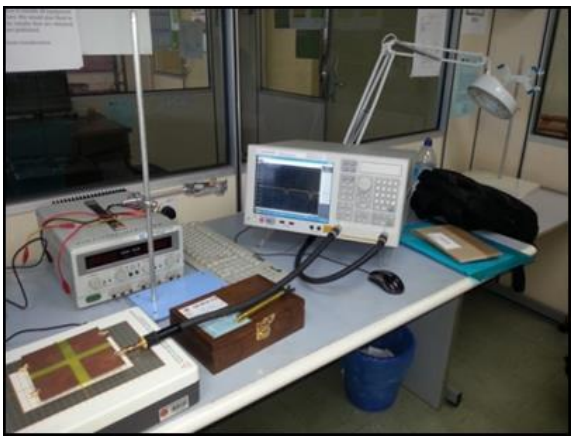

(c)

Figure 7: MIMO four port antenna prototype with (a) Front View, (b) Rear View and (c) Performing Measurement

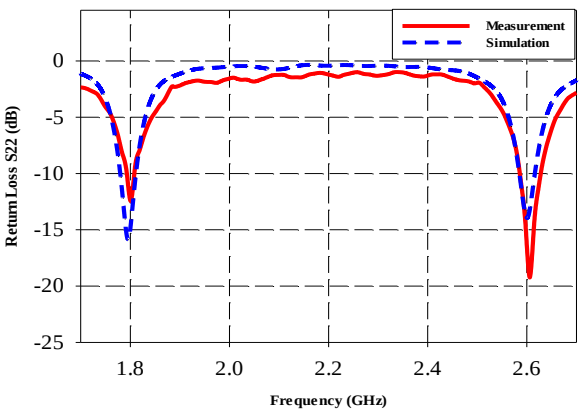

Figure 8: Comparison of simulation results with the measurement at Port 2 (S_{22}).

In Figure 9, the measured antenna return loss for mutual couplings is compared with the simulated results. The coupling level for the measured result is observed to be poorer than the simulation. The experimental value exhibits a resonance of 39% and the achieved bandwidth for the prototype is found to be higher accompanied by upward shift from1.8GHz to1.845 GHz. Slight disagreements between the measured and simulated results have been observed.

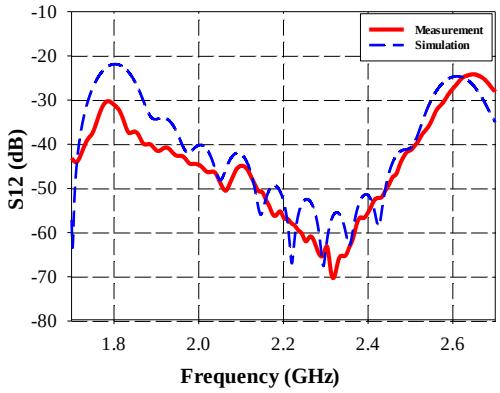

Figure 9: Comparison of simulation results with measurement for mutual coupling S_{12}.

The disagreements between the measured and simulated results for S_{14} and S_{13} parameters are illustrated in Figure 10 and 11, respectively.

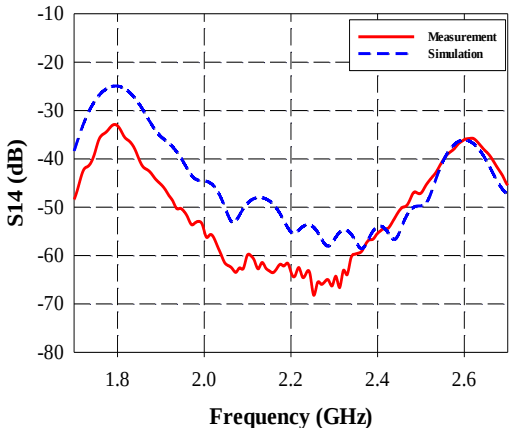

Figure 10: Comparison of simulation results with the measurement for mutual coupling S_{14}

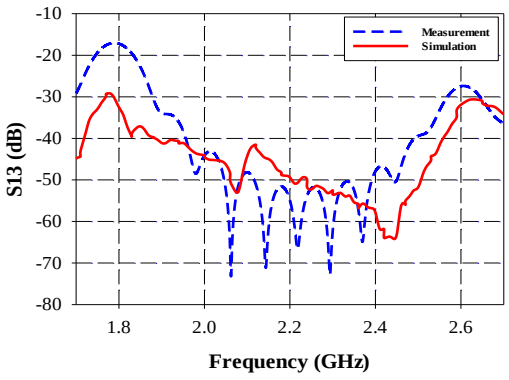

Figure 11: Comparison of simulation results with the measurement for mutual coupling S_{13}.

Following equations relating *S*-parameters and normalized mutual resistances of the 4-ports MIMO are used to calculate the correlation coefficients (CCs) [17].

$$\rho_e(i,j) = \rho_s(i,j) = \frac{\left|\sum_{m=1}^{M} S_{i,m}^{*} S_{m,j}\right|^2}{\prod_{k=i,j}\left[1-\sum_{m=1}^{M} S_{k,m}^{*} S_{m,k}\right]} \quad (1)$$

$$\rho_e(i,j) = \left|\rho_r(i,j)\right|^2 \cong \left|r_{i,j}\right|^2 = \frac{\left|R_e(Z_{i,j})\right|^2}{\left|R_e(Z_{i,i})\right|} \quad (2)$$

$$\rho_e(1,2) = \frac{\left|S_{11}^{*}S_{12} + S_{12}^{*}S_{22} + S_{13}^{*}S_{32} + S_{14}^{*}S_{42}\right|^2}{\left(1-\left(S_{11}^{*}S_{11} + S_{12}^{*}S_{21} + S_{13}^{*}S_{31} + S_{14}^{*}S_{41}\right)\right)\left(1-\left(S_{21}^{*}S_{12} + S_{21}^{*}S_{22} + S_{23}^{*}S_{32} + S_{24}^{*}S_{42}\right)\right)} \quad (3)$$

where $\rho_e(i,j)$ is CC or mutual coupling between element, M is the number of ports, K is the number of elements and Z_{ij} is the impedance. Simulation results as illustrated in Figure 12 demonstrate the achieved superior CCs between the two ports with $\rho_e(1,2) \approx 0$ for *S*-parameters and $\rho_e(1,2) > 0.008$ for normalized mutual resistances. The measured CCs reveal consistent behavior with $\rho_e(1,2)$ less than 0.01 for S-parameters and 0.125 for normalized mutual resistances.

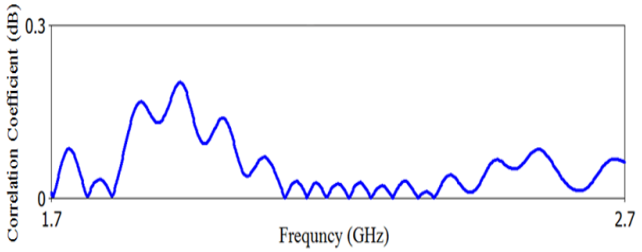

Figure 12: Envelope correlation coefficients for the four-port MIMO obtained using *S*-parameters and normalized mutual resistances.

The correlation coefficients at resonance frequency are calculated using the discrete component values of 3D radiation patterns from CST microwave studio simulation, measured S-parameters and normalized mutual resistances as listed in Table 3. Very good agreement between measured and simulated results is achieved. The simulated and measured values of envelope correlation coefficient occurring below the diversity performance ($\rho s < 0.5$) demonstrate that our newly designed four-port MIMO provides a good diversity as the multiport antenna. The simulation results as shown in Figure 13 displays excellent correlation coefficients between the two ports $\rho_e(1,3) \approx 0$ for S-parameters and $\rho_e(1,3) > 0.005$ for normalized mutual resistances.

Table 3
Comparison of CCs for S-Parameters at 1.8GHZ.

Correlation Coefficients for S-Parameter	Simulation	Measurement	Differences
$\rho_s(1,2)$	0.0397	0.0445	-0.0048
$\rho_s(1,3)$	0.0397	0.0498	-0.0101
$\rho_s(1,4)$	0.0240	0.0284	-0.0044
$\rho_s(2,1)$	0.0240	0.0333	-0.0093
$\rho_s(2,3)$	0.0240	0.0458	-0.0218
$\rho_s(2,4)$	0.0271	0.0441	-0.0170
$\rho_s(3,1)$	0.0426	0.0912	-0.0486
$\rho_s(3,2)$	0.0232	0.0254	-0.0022
$\rho_s(3,4)$	0.0222	0.0315	-0.0093
$\rho_s(4,1)$	0.0232	0.0285	-0.0053
$\rho_s(4,2)$	0.0259	0.0421	-0.0162
$\rho_s(4,3)$	0.0160	0.0321	-0.0161

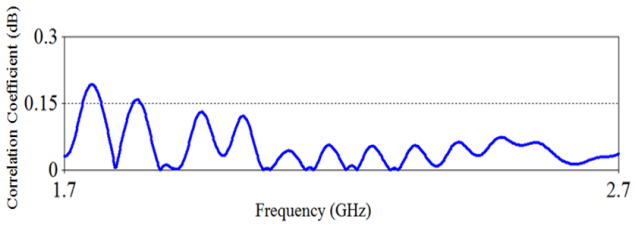

Figure 13: Envelope correlation coefficients for the four-port MIMO using S-parameters $\rho_e(1,3)$ and normalized mutual resistances $\rho_e(1,3)$.

The CCs as depicted in Figure 14 and 15 are calculated directly from the measured S-parameters follow the similar pattern with the simulated ones. This is due to the slightly overestimate of the port isolation (0.09124) in comparison to the simulated value of 0.042694. The normalized mutual impedance obtained from the measured *S*-parameters produce low CCs similar to their simulated counterparts but possess higher fluctuations. This difference in fluctuations is ascribed to the modified phase patterns influenced by slightly different lengths of coaxial cables used for connection to excite the antenna. However, the CC values obtained from both the simulation and measurement are low enough (0.5) to yield effective diversity performance.

The diversity performance of the multiport CDRAs is evaluated and MIMO performance benchmarking such as matched ports, high isolation (low mutual coupling), different feed radiation pattern and polarization directions, low correlation coefficients between ports (preferably less than 0.5) and similar MEG in each branch are performed. A diversity gains of 10 dB for the four-ports MIMO using *S*-parameters S_{12} and S_{24} as shown in Figure 16 and 17, respectively. The evaluation employs *S*-parameters and radiation patterns results from CST microwave studio simulation and real experiment using Agilent Technologies E5071B VNA and an anechoic chamber. Table 4 enlists the comparison of the simulated and measured values of diversity gain for the four-port MIMO using *S*-parameters.

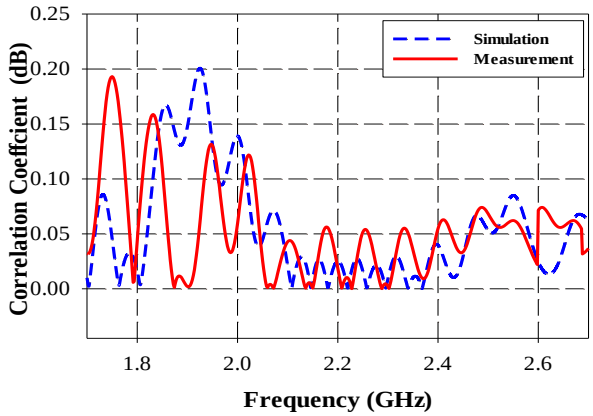

Figure 14: Comparison of envelope CCs for the four-port MIMO using S-Parameters $\rho_e(1,2)$.

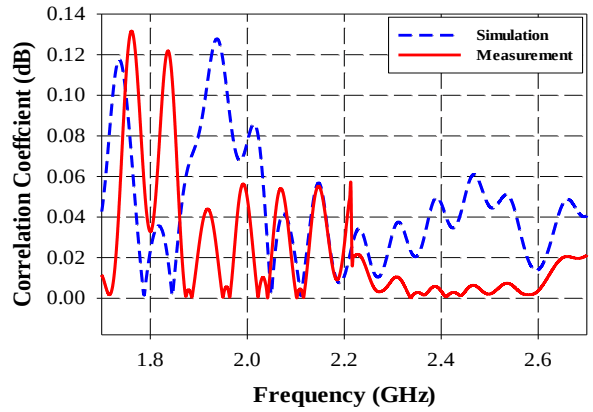

Figure 15: Comparison of envelope CCs for the four-port MIMO using *S*-Parameters $\rho_e(2,3)$.

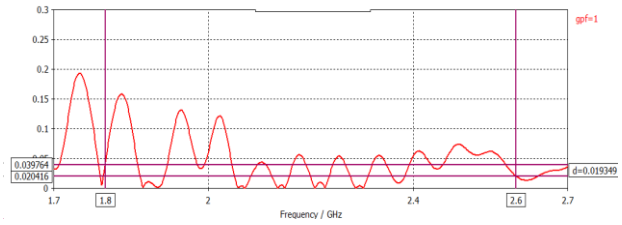

Figure 16: Diversity gain of 10 dB for the four-port MIMO obtained using *S*-parameters S_{12}.

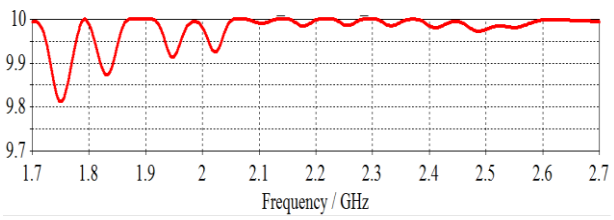

Figure 17: Diversity gain of 10 dB for the four-port MIMO obtained using *S*-parameters S_{13}.

Table 4
Comparison of CCs for S-Parameters at 2.6GHZ

Correlation Coefficients for S- Parameter	Simulation	Measurement	Differences
$\rho_s(1,2)$	0.02041	0.02994	-0.00953
$\rho_s(1,3)$	0.02041	0.03254	-0.01213
$\rho_s(1,4)$	0.00363	0.02548	-0.02185
$\rho_s(2,1)$	0.00363	0.02765	-0.02402
$\rho_s(2,3)$	0.01372	0.02245	-0.00873
$\rho_s(2,4)$	0.01634	0.03454	-0.01820
$\rho_s(3,1)$	0.01968	0.07200	-0.05232
$\rho_s(3,2)$	0.01363	0.01900	-0.00537
$\rho_s(3,4)$	0.01710	0.01900	-0.00190
$\rho_s(4,1)$	0.03628	0.03800	-0.00172
$\rho_s(4,2)$	0.01626	0.02500	-0.00874
$\rho_s(4,3)$	0.02214	0.04100	-0.01886

The diversity gain of the MIMO antenna for four ports is calculated using the equations [16],

$$G_{app} = 10e_p \tag{4}$$

$$e_p = \sqrt{(1-|0.99\rho|^2)} \tag{5}$$

where 10 is the maximum apparent diversity gain at the 1% probability level with selection combining, and e_ρ is an approximate expression for the correlation efficiency which is the reduction in diversity gain due to the correlation between the signals on the two branches. This formula is not very accurate for correlations close to unity when compared with the more accurate formulas. In table 5 and 6 Measured values of diversity gain for the four-port MIMO using S-parameters are compared with simulation results at 1.8 GHz and 2.6GHz respectively. However, scaling ρ with a factor 0.99 much more accurate results can be obtained.

A maximum apparent diversity gain of 10 at the 1% probability level with selection combining G_{app} and an approximate expression for the correlation efficiency (e_p) is achieved.

Table 5
Measured Values of Diversity Gain for the Four-Port MIMO Using S-Parameters are Compared with Simulation Results at 1.8 GHz.

Correlation Coefficients for S-Parameter	Simulation	Measurement	Differences
$\rho_s(1,2)$	0.039764	0.046085	-0.00632
$\rho_s(1,3)$	0.039764	0.046085	-0.00632
$\rho_s(1,4)$	0.024002	0.02841	-0.00441
$\rho_s(2,1)$	0.024002	0.03331	-0.00931
$\rho_s(2,3)$	0.024002	0.02587	-0.00187
$\rho_s(2,4)$	0.027100	0.04412	-0.01702
$\rho_s(3,1)$	0.042694	0.04994	-0.00725
$\rho_s(3,2)$	0.023211	0.02548	-0.00227
$\rho_s(3,4)$	0.022238	0.03154	-0.00930
$\rho_s(4,1)$	0.023213	0.02854	-0.00533
$\rho_s(4,2)$	0.025937	0.04214	-0.01620
$\rho_s(4,3)$	0.016264	0.03214	-0.01588

Table 6
Measured Values of Diversity Gain for the Four-Port MIMO USING S-Parameters are Compared with Simulation Results at 2.6GHz

Correlation Coefficients for S- Parameter	Simulation	Measurement	Differences
$\rho_s(1,2)$	0.020416	0.03514	-0.01472
$\rho_s(1,3)$	0.020416	0.03514	-0.01472
$\rho_s(1,4)$	0.0036392	0.02548	-0.02184
$\rho_s(2,1)$	0.0036392	0.02765	-0.02401
$\rho_s(2,3)$	0.013726	0.01245	0.001276
$\rho_s(2,4)$	0.01634	0.03454	-0.01820
$\rho_s(3,1)$	0.01968	0.03954	-0.01986
$\rho_s(3,2)$	0.01363	0.01958	-0.00595
$\rho_s(3,4)$	0.017108	0.01965	-0.00254
$\rho_s(4,1)$	0.036287	0.03874	-0.00245
$\rho_s(4,2)$	0.016264	0.02540	-0.00914
$\rho_s(4,3)$	0.022144	0.03156	-0.00942

The simulated radiation pattern is as presented in Figure 18. The simulated HPBW for E-field is 84.7deg at 1.8GHz and 80.8deg at 2.6GHz while the HPBW for H field is 93.9deg at 1.8GHz and 59deg at 2.6.The Gain for the1.8GHz and 2.6GHz is 3.969 dBi and 3.22dBi respectively. The measured radiation pattern is illustrated in Figure 19

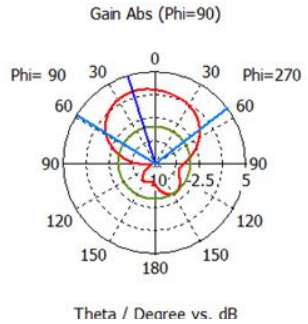

Figure 18: Radiation pattern for 1st Band 1.8 GHz for MIMO antenna

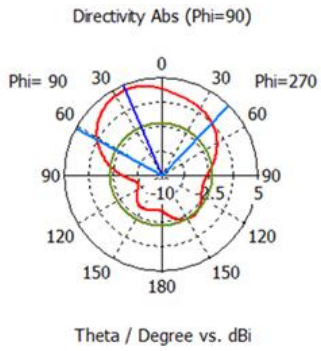

Figure 19: Radiation pattern for 2nd Band 2.6 GHz for MIMO antenna

V. CONCLUSION

A four ports MIMO antenna is designed and implemented to achieve efficient bandwidth broadening. The characteristic evaluation of four ports dual-band MIMO antenna based on a microstrip patch operating at 1.8 and 2.6 GHz is performed. The fabricated antenna is tested via experiment and simulation. The designed antenna has the small ground plane, and low mutual coupling is found to be potential for LTE applications. Superior diversity performance of the antenna is in terms of enveloping CCs and diversity gain is demonstrated. The simulated and measured results showed good agreement. An excellent pattern diversity, low correlation coefficient, high gain, superior directivity, and quite reasonable bandwidth in the above-mentioned range is achieved which is suitable for LTE bands application. Simulation is performed via CST microwave studio program, and experimental measurements are performed through Agilent Technologies E5071B VNA and the anechoic chamber. Our new design and performance assessment of the MIMO antenna may contribute towards the development of LTE applications.

ACKNOWLEDGMENTS

This work is fully sponsored by Universiti Teknikal Malaysia Melaka (UTeM) Postgraduate Zamalah Scheme, 2018.

REFERENCES

[1] Kyeong-Sik Min, Dong-Jin Kim, Min-Seong Kim,'' Multi-channel MIMO Antenna Design for WiBro/PCS band,'' IEEE, 2007. 1-4244-0878-4/07
[2] Garg, R., Bhartia, P., Bahl, I., Ittipiboon, A., Microstrip Antenna Design Handbook, Artech House, Inc. 2001.
[3] Kumar, G. and Ray, K.P., Broadband Microstrip Antennas, Artech House, Inc. 2003.
[4] O. Claude, Bruno Clerckx, "MIMO Wireless Communications," Elsevier Ltd. California, USA,2007. p1-3.
[5] Kyeong-Sik Min, Dong-Jin Kim, Min-Seong Kim,'' Multi-channel MIMO Antenna Design for WiBro/PCS band,'' IEEE, 2007. 1-4244-0878-4/07.
[6] Jun Tong, Peter J. Schreier, Senior, Steven R. Weller, "Design and Analysis of Large MIMO Systems With Krylov Subspace Receivers," IEEE, 2012. VOL. 60, NO. 5.
[7] Rao, P. V. V. K., Vishnu, C., Reddy, V., Tejaswini, K., Babu, B. V. V. R., Babu, K. J. ,"A Wideband H Shape Dielectric Resonator Antenna for Wireless MIMO Systems," 2012. 1(3), 64-66.
[8] Rezaei, P, Hakkak, M, Forooraghi, K. ,"Design of Wide-Band Dielectric Resonator Antenna With a Two-Segment Structure," Progress In Electromagnetic Research, 2006. 66, 111-124. doi:10.2528/PIER06110701
[9] Garg, R., Bhartia, P., Bahl, I., Ittipiboon, A., Microstrip Antenna Design Handbook, Artech House, Inc. 2001.
[10] Ishimiya, K, Ying, Z, Takada, J.-ichi,"A Compact MIMO DRA for 802. 11n application,"2008. 1(1), 4-7.
[11] D. Franco, J. Lluis,"Multi-antenna Systems for MIMO Communications,". Morgan and Claypool Publishers, 2008. Arizona, 8-12.
[12] John Wiley, Sons Inc Constantine, A.Balanis, "Antenna Theory, Analysis and Design," publication, 2005. 3rd ed., pg.813.
[13] Kyeong-Sik Min, Dong-Jin Kim, Min-Seong Kim,'' Multi-channel MIMO Antenna Design for WiBro/PCS band,'' IEEE, 2007. 1-4244-0878-4/07.
[14] L, P. R,"A review on the design of MIMO antennas for upcoming 4G,"2011. 1(4), 85-93.
[15] Ezio Biglieri, Robert Calderbank, Anthony Constant inides, Andrea Goldsmith, Arogy as wami Paulraj, H. Vincent Poor,"MIMO Wireless Communications," Cambridge University Press. New York,2007. P 1-3.
[16] Yu-Chun Lu, Yao-Chia Chan, Hsueh-JyhLi, Yi-Cheng Lin, Shun-Chang Lo, Gene C.-H. Chuan," Design and System Performances of A Dual-Band 4-Port MIMO Antenna for LTE,''IEEE,2011.978-1-4244-
[17] KO S.C.K., MURCH R.D.: 'Compact integrated diversity antenna for wireless communications', IEEE Trans. Antennas Propag., 2001, 49, (6), pp. 954–960